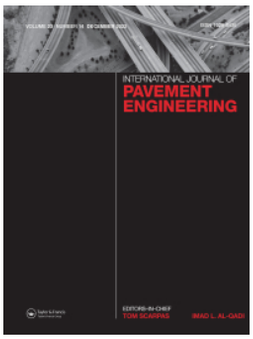

International Journal of Pavement Engineering

ISSN: (Print) (Online) Journal homepage: www.tandfonline.com/journals/gpav20

Evaluation of the electrochemical interaction in the asphalt emulsion-aggregate system of cold mix asphalt through zeta potential and surface free energy analysis

Z. I. Cuaran-Cuaran, Miguel Castilla-Barbosa, Orlando Rincón & Manuel Ocampo-Terreros

To cite this article: Z. I. Cuaran-Cuaran, Miguel Castilla-Barbosa, Orlando Rincón & Manuel Ocampo-Terreros (2024) Evaluation of the electrochemical interaction in the asphalt emulsion-aggregate system of cold mix asphalt through zeta potential and surface free energy analysis, International Journal of Pavement Engineering, 25:1, 2361837, DOI: 10.1080/10298436.2024.2361837

To link to this article: https://doi.org/10.1080/10298436.2024.2361837

Published online: 10 Jun 2024.

INTERNATIONAL JOURNAL OF PAVEMENT ENGINEERING
2024, VOL. 25, NO. 1, 2361837
https://doi.org/10.1080/10298436.2024.2361837

Evaluation of the electrochemical interaction in the asphalt emulsion-aggregate system of cold mix asphalt through zeta potential and surface free energy analysis

Z. I. Cuaran-Cuaran[a], Miguel Castilla-Barbosa[a], Orlando Rincón[b] and Manuel Ocampo-Terreros[a]

[a]Department of Civil Engineering, Pontificia Universidad Javeriana, Bogotá D.C., Colombia; [b]Infrastructure Division, WSP Colombia, Bogotá D.C., Colombia

ABSTRACT

The interaction in the emulsion-aggregate system is well known and influences the Cold Mix Asphalt (CMA) performance. However, the electrochemical interaction indexes for the emulsion-aggregate systems are still not well understood. Therefore, the present investigation focussed on evaluating the electrochemical interaction in the Asphalt Emulsion-Aggregate system (AEA-S) of Cold Mix Asphalt (CMA). Zeta Potential (ZP), X-ray diffraction (XRD), and Surface Free Energy (SFE) analysis were carried out in three slow-setting cationic asphalt emulsions and three common Colombian aggregates (alluvial and quarried) to determine the electrical potential and interaction in the emulsion-aggregate system. Zeta Potential analysis shows both dependence on the chemical compounds of the aggregates and variation in pH conditions. Moreover, Zeta Potential shows negative values for all three aggregates in the entire pH range variation and decreases with asphalt emulsions pH associated with SiO_2/Al_2O_3 ratio. Through chemical identification and electrokinetic forces is feasible to conclude that high Zeta Potential (ZP) and Surface Free Energy (SFE) values improve the electrochemical ad of the asphalt emulsion-aggregate system (AEA-S), demonstrating that high polarity is an essential factor in Cold Mix Asphalts (CMA).

ARTICLE HISTORY
Received 1 September 2023
Accepted 24 May 2024

KEYWORDS
Cold mix asphalt; asphalt emulsion-aggregate interaction; residual asphalt-aggregate interaction; surface free energy; zeta potential

1. Introduction

The enhancement of Cold Mix Asphalt (CMA) performance has been a focal point of research globally over the past three decades. This attention stems primarily from its historically subpar performance relative to Hot Mix Asphalt (HMA), as well as the desire to leverage its environmental and economic advantages to establish it as a dependable technology for roads subjected to high-density traffic (Dash *et al.* 2022, Day *et al.* 2019, Doyle *et al.* 2013, Jain and Singh 2021, Lastra-González *et al.* 2019, Saadoon *et al.* 2017, Shanbara *et al.* 2021).

In Colombia, there has been a recent emphasis on the implementation of Cold Mix Asphalt (CMA), driven by increased interest from governmental agencies. This interest has surged in response to observed premature pavement failures on certain highway projects during the 1990s. The growing interest in CMA aims to promote more sustainable practices within the construction industry, which has traditionally favoured Hot Mix Asphalt (HMA) despite potential drawbacks related to climatic conditions. Consequently, several infrastructure agencies have begun to advocate for the adoption of new technical specifications to encourage the use of CMA in major roadways.

These changes in technical regulations necessitate the development of studies aimed at enhancing CMA applications. One crucial aspect to consider is the electrochemical interaction between Asphalt Emulsion (AE) and aggregate, as this interaction significantly influences CMA performance and poses a challenge due to various factors affecting the Asphalt Emulsion breaking process (Cardone *et al.* 2018, Gorman *et al.* 1998, Graziani *et al.* 2018, Khan *et al.* 2016a). Additionally, the interaction between binders and aggregates plays a several role in determining asphalt mixture performance (Boulangé *et al.* 2013, Gorman *et al.* 1998, Guo *et al.* 2020, 2018, Khan *et al.* 2016b, Labib 1992, Júnior *et al.* 2019, Miller *et al.* 2012).

Several kinds of research have been conducted to understand how this interaction works on Hot Mix Asphalt (HMA) and which characteristics affect mechanical mix response at the macroscopic scale (Graziani *et al.* 2018, Jain and Singh 2021, Khan *et al.* 2016a, Lee and Ahn 2016, Ziyani *et al.* 2016). Furthermore, those studies have analysed the interaction between the Residual Asphalt (RA) and the aggregate concluding that the performance differences of CMA concerning HMA are generally associated with the interaction of the Asphalt Emulsion-Aggregate System (AEA-S). However, those studies have not represented the behaviour of the residual asphalt from the Asphalt Emulsion (AE) breaking when it mixes with the aggregate. On the other hand, few studies have analysed the electrochemical interaction of the AEA-S in the CMA preparation stage (Gorman *et al.* 1998, Lee and Ahn 2016, Wates and James 1993, Ziyani *et al.* 2016). Those studies do not involve the AE breaking process which results in the resultant force between the Residual Asphalt (RA) and the aggregate.

The measurement of zeta potential and sessile drop (related to surface free energy) has garnered significant interest as a means to ascertain the surface electric charge of asphalt and

CONTACT Miguel Castilla-Barbosa castilla.m@javeriana.edu.co

asphalt-aggregate emulsions. These measurements serve to investigate the electrostatic interaction within emulsion-aggregate or asphalt-aggregate systems, offering insights into compatibility, adhesion strength, and the phenomenon of moisture damage, as well as shedding light on the breaking mechanism and stability of asphalt emulsions (Thanaya 2003, Gorman *et al.* 1998, Lee and Ahn 2016, Needham 1996, Wates and James 1993, Labib 1992, Khan *et al.* 2016a, Ziyani *et al.* 2016, Wei and Zhang 2012). However, despite extensive research, the understanding of electrochemical interactions in terms of electric charge and surface free energy remains incomplete.

Consequently, the present study aims to assess the Asphalt Emulsion-Aggregate System (AEA-S) using Colombian pavement materials through the Zeta Potential (ZP) test and Surface Free Energy (SFE) technique, with a particular emphasis on the asphalt emulsion breaking process. To achieve this, three slow-setting cationic asphalt emulsions and three aggregate sources (two of alluvial origin and one quarried) were subjected to evaluation at the micro-scale level.

2. Background

Several studies have focussed on understanding the phenomena and factors involved in the binder-aggregate system interaction to predict asphalt mixture performance (Gorman *et al.* 1998, Khan *et al.* 2016a, 2016b, Guo *et al.* 2020, Labib 1992, Júnior *et al.* 2019, Miller *et al.* 2012). Regarding the performance differences between cold mix asphalt (CMA) and hot mix asphalt (HMA), they are often associated with the interaction of the emulsion-aggregate system, as indicated in different studies (Ziyani *et al.* 2016, Graziani *et al.* 2018, Jain and Singh 2021, Khan *et al.* 2016a). They have primarily analysed the interaction between residual asphalt (RA) and aggregate.

However, the residual asphalht (RA) studied has not represented the real conditions of RA resulting from the spontaneous breaking of asphalt emulsion when mixed with the aggregate. Furthermore, few studies (Gorman *et al.* 1998, Lee and Ahn 2016, Ziyani *et al.* 2016, Pinto and Buss 2020) have analysed the interfacial performance in the initial stage of CMA preparation, where the asphalt emulsion comes into contact with the aggregate to initiate the breaking process. Some approaches to evaluate the interfacial performance of the emulsion-aggregate system have been carried out using techniques such as surface energy (SFE) and zeta potential to determine the surface properties of the asphalt emulsion and aggregate that influence their interaction. Consequently, a lack of parameters to define the interfacial performance or compatible state developed by the emulsion-aggregate system in terms of zeta potential and surface free energy has been identified.

As aforementioned, optimising asphalt pavement performance, the compatibility between residual asphalt (RA) and aggregates plays a relevant role. In the first instance, in 2018, Graziani *et al.* (2018) investigated adhesion strength using the BBS test between residual asphalt (RA), obtained via the evaporation method, and two aggregate types (limestone and basalt). However, despite considering variables like curing time and temperature, the study found adhesion failure between the RA and aggregate, indicating an unsatisfactory indication of compatibility between the materials.

Ling *et al.* (2016) investigated the adhesion strength between the RA and aggregate, alongside preparations of CMA to compare aggregate coverage by the RA pre and post boiling test. Additionally, they evaluated mixtures for tensile strength under dry and wet conditions to assess moisture susceptibility based on the tensile strength ratio. However, this qualitative approach did not fully elucidate the compatible state between the RA and aggregate. A similar focus on RA evaluation is noted in the study of Graziani *et al.* (2018). Furthermore, Ziyani *et al.* (2016) examined surface properties such as surface tension and energy of cationic asphalt emulsions and minerals (gneiss, diorite, limestone, and quartzite), while also exploring the adhesion work of emulsion-mineral systems. They observed strong compatibility between emulsions and minerals, suggesting their suitability for CMA preparation. Despite this insightful analysis, further macro-scale evaluations are needed to comprehensively understand the interfacial performance between asphalt emulsion and aggregate. Similarly, Khan *et al.* (2016a) characterised surface properties of minerals/aggregates and emulsified asphalt grades for CMA, albeit using asphalt that did not accurately represent the conditions of RA characteristic of asphalt emulsion.

On the other hand, there has been an interest in the surface electrical charge, which is a relevant property in CMA materials as aforementioned. Lee and Ahn (2016) aimed to assess the interaction between aggregates (trap rock, Mondoñedo Quarry aggregates, blast furnace slag, steel slag, limestone, dolomite, and gravel) and emulsions (CRS-2P, RS-2P, and AE-90S) in terms of surface electrical charge, also known as zeta potential, as it relates to material attraction. They also conducted tests for aggregate loss and curing. It was observed that the zeta potential (as a function of pH) of an aggregate was negative at both low and high pH levels, indicating an attraction interaction with asphalt emulsions that exhibited a positive zeta potential (CRS-2P).

Gorman *et al.* (1998) examined the emulsion aggregate system, characterising aggregates based on zeta potential, contact angle, and qualitative tests of mixing time and cohesion. They found that aggregates with hydrophobic surfaces (Washburn contact angle $\geq 68.1^{\circ}$) are suitable for pavement surface treatments (Slurry). Similarly, Wates and James (1993) investigated zeta potential measurements on asphalt emulsions and aggregates, finding that acidic aggregates or those with a negative zeta potential are compatible with cationic asphalt emulsions, promoting strong adhesion. Conversely, basic aggregates or those with a positive to neutral zeta potential are expected to exhibit the opposite behaviour. Furthermore, a positive zeta potential in asphalt emulsions is linked to rapid breaking during mixing. However, it was noted that the results of zeta potential and contact angle were not validated with strength tests, hindering the assessment of interfacial performance between asphalt emulsion and aggregate.

Likewise, it has been found that the evaluation of the adhesion property with the asphalt emulsion has made use of the SFE theory, evaluating mostly contact angles using the asphalt residue (Wang *et al.* 2020, Alvarez *et al.* 2019), emulsified asphalts (Han *et al.* 2019, Tan *et al.* 2022, Du

et al. 2023), or the asphalt emulsion (Wang *et al.* 2020, Meng *et al.* 2023), and in some cases the SFE (Liu *et al.* 2020, Tang *et al.* 2018). Hence, this indicates that the evaluation of SFE on asphalt emulsions is limited, generating the need for further characterisation of this property to further understand the adhesion at the interface of the asphalt emulsion and aggregate.

3. Materials and methods

3.1. Specimen selection

Asphalt emulsions are commonly used to produce bound granular materials for structural layers in pavements. Asphalt emulsions are characterised by two relevant factors: their charge (cationic or anionic) and their setting or breaking speed (slow, medium, and quick). The charge in an asphalt emulsion will be opposite to the charge of the granular material, and the choice of setting will depend on the application. Cationic emulsions are more frequently used as the common negative charge of soils and granular materials. A cationic slow-setting (CSS) is primarily used for dense graded cold mix asphalt (dense CMA), for full-depth reclamation (FDR) to improvement soils in pavement rehabilitations, and cold in-place recycling (CIR) of the reclaimed asphalt pavement (RAP); a cationic medium-setting (CMS) is typically used for open graded cold mix asphalt (open CMA); and a cationic quick-setting (SQS) is primarily used for spray applications such as chip seals and scrub seals (Casillas and Braham 2022).

As aforementioned, slow setting emulsions are characterised by their longer breaking and setting times, which make them ideal for worldwide dense graded mixtures, where thorough coating and penetration into the aggregate are necessary. In this way, in the current investigation three slow-setting cationic (CSS) Asphalt Emulsions were utilised to assess the performance of Cold Mix Asphalt (CMA): CSS-1, CSS-1h, and CSS-1 SF (special formulation). The designation 'h' denotes high stability asphalt emulsions. CSS-1 and CSS-1h emulsions are currently standardised by the Colombian highways agency for applications such as Prime Coat and Slurry Seal. Conversely, CSS-1 SF represents a modified asphalt emulsion with alterations in particle diameter. In addition, all the asphalt emulsions (AE) used in this study were provided by a certified supplier. They were made using a single type of Colombian asphalt and different proportions of the same emulsifier were used in their manufacture. Hence, it is essential to note that these emulsions were meticulously selected to ensure consistency and comparability of the results in our analysis.

On the other hand, The selection of three aggregate sources–Coello River (CR), Guayuriba River (GR), and Mondoñedo Quarry (MQ)–was based on their geological composition, with CR aggregates predominantly comprising igneous and metamorphic materials, while GR and MQ consist mainly of sedimentary materials (Figure 1).

3.2. Zeta potential analysis

As stated (Salopek *et al.* 1992), Zeta Potential (ZP) or Electrokinetic Potential represents an electrical property of an interface, whether solid or liquid. Consequently, ZP serves as a relative measure of electric charge, employing the particle electrophoretic mobility technique. This technique applies an electric field to charged particles in dispersion, measuring particle velocity as electrophoretic mobility (Castilla-Barbosa *et al.* 2023). In this context, ZP is determined using the equation proposed by Smoluchowski, as shown in Equation (1), where μ_E denotes electrophoretic mobility, ε represents the permittivity of the dispersion medium, ζ signifies ZP, and η denotes the viscosity of the dispersion medium.

$$\mu_E = \frac{\upsilon\zeta}{\eta} \tag{1}$$

Additionally, Zeta Potential (ZP) is significantly influenced by the dispersion medium, pH level, and particle surface composition. Consequently, various concentrations of H^+ and OH^- ions were employed to determine their capacity to neutralise, diminish, or augment particle ZP, as suggested by Guo *et al.* (2020), Lee and Ahn (2016) and Needham (1996). Moreover, concerning surface composition, particles may ionise in the dispersion medium, acquiring either a positive or negative charge. In broader terms, ZP pertains to a colloidal system that maintains stability due to repulsive forces generated between dispersed particles sharing the same electrical charge (+) (Thanaya 2003). Higher ZP values (+) of dispersed particles indicate stronger repulsive forces, thereby hindering their flocculation, while lower ZP values (+) suggest weaker repulsive forces, resulting in flocculation (Malvern 2015). Furthermore, ZP can range from 0 to 100 millivolts to assess the distinction between a stable and an unstable system (Dukhin and Xu 2020), with values typically exceeding +30 mV or −30 mV to ensure stability (Malvern 2015, Thanaya 2003).

To guarantee the representativeness of the aggregates a classification process was developed through visual sieving to define the clastic distribution based on the Munsell colour charts to define the most representative three fractions (based on colour which implies changes in chemical compounds). On this way, Coello River aggregates exhibit 5B 5/1, 10R 7/4, 5B 7/1 clasification based on Munsell Color chart, Guayuriba River 7.5R 6/2, 10Y 2, N5, and Mondoñedo Quarry 5Y 8/1, 10YR 8/6, 10YR 8/2. Afterward, compositional verification was executed through Scanning Electron Microscopy (SEM), and the most significant fractions were selected for Zeta Potential analysis. It is important to highlight that the preliminary Zeta Potential analysis did not show relevant differences between the three relevant fractions of Guayuriba River aggregates. Thus, a mix of representative fractions was used for the Zeta Potential test.

Furthermore, all aggregates underwent a series of preparation steps to ensure uniformity and suitability for analysis. This included sieving using a 4.75 mm mesh, followed by washing with distilled water, and subsequent drying in an oven at 110°C for 24 h. Additionally, the aggregates underwent crushing and further sieving using a 0.075 mm mesh to homogenise the materials and achieve the required particle size for the Zeta Potential (ZP) test, given its significant influence on the analysis (Guo *et al.* 2020).

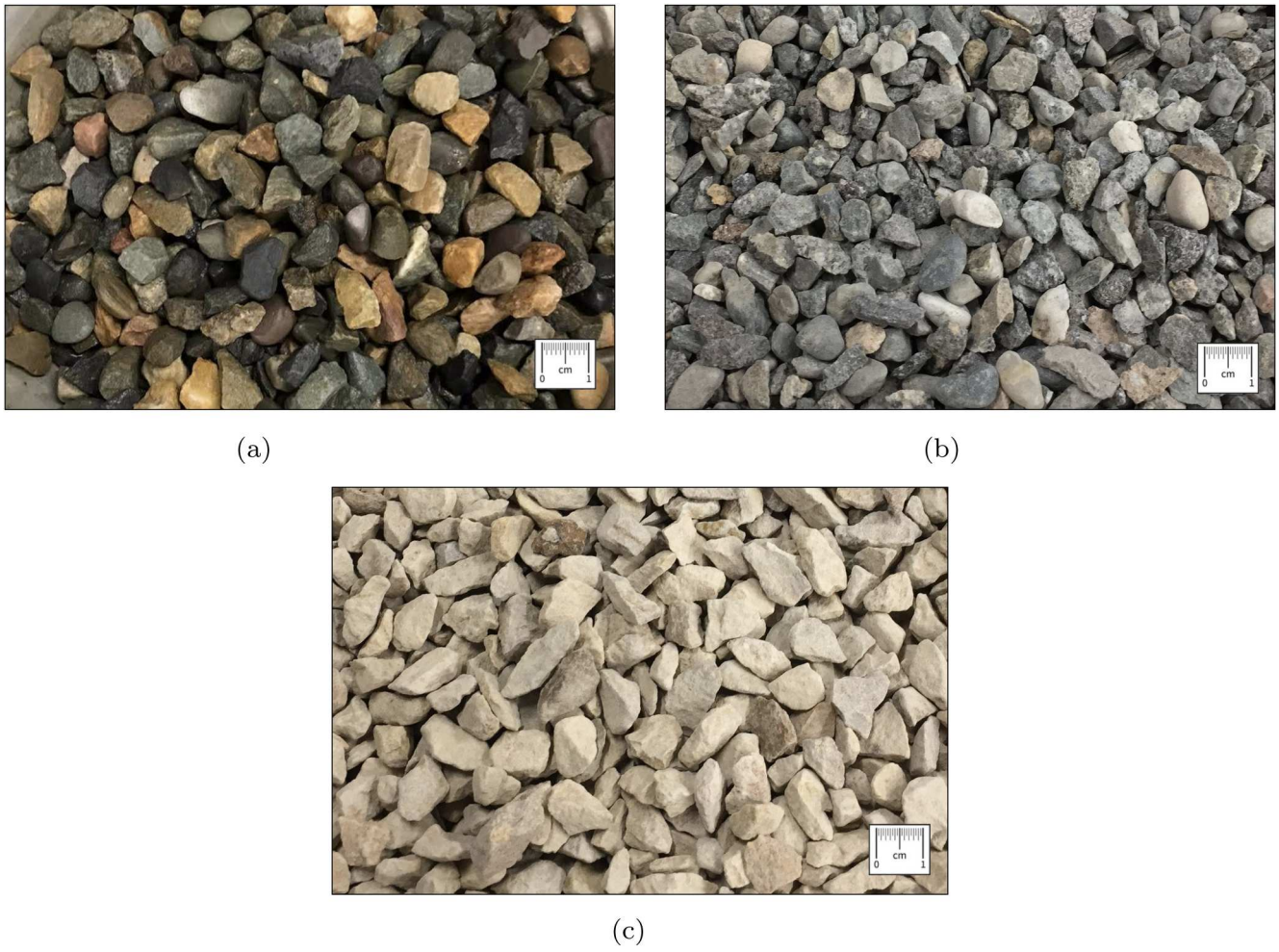

Figure 1. Aggregates of Coello (CR) and Guayuriba River (GR), and Mondoñedo Quarry (MQ) under study. (a) Guayuriba River (GR) aggregates. (b) Coello River (CR) aggregates and (c) Mondoñedo Quarry (MQ) aggregates.

The particle size distribution of the crushed fractions was then determined through laser granulometry using a Mastersizer 3000E granulometer, identifying the d_{10}, d_{50}, and d_{90}. In the initial analysis, the d50 values were found to be 24.6 m for Coello River, 20 μm for Guayuriba River, and 29.7 m for Mondoñedo Quarry. Similarly, the d10 values were measured at 3.34 m for Coello River, 2.70 m for Guayuriba River, and 2.54 m for Mondoñedo Quarry. Subsequently, all ZP tests for both aggregates and Asphalt Emulsion were carried out using a Zetasizer Nano Series (ZS90) (Malvern 2015). It is relevant to highlight that the determination of the d_{50} was considered as a crucial descriptor in particle classification, representing the median particle size and providing valuable insights into the sample's average particle size. Laser granulometers, whether monomodal or multimodal, are commonly employed for particle size analysis due to their accuracy and efficiency. These instruments utilise light scattering techniques to measure particle size distribution, ensuring precise control over particle distribution within the sample.

The Asphalt Emulsion (AE) and aggregates underwent dissolution in deionised water with varying pH levels ranging from 2 to 9. Notably, the pH levels from 2 to 5 were adjusted using HCl (0.001 M), while pH 8 and 9 were adjusted using NaOH (0.001 M), as prescribed by ASTM E2865 standard and recommended by Lee and Ahn (2016). This pH range selection was deliberate: pH 2 and 2.5 corresponded to Asphalt Emulsion pH levels, 5 and 7 represented the aqueous environment for Cold Mix Asphalt preparation, and 8 and 9 reflected the pH levels of the aggregates. For the Zeta Potential analysis of both the AE and aggregates, 5 l of AE was dissolved in 40 ml of deionised water, while 0.014 g of aggregate was dissolved in 10 ml of water (see Figure 2). ZP analysis was conducted with 10 Zeta runs per pH and per sample, with 250 internal subruns per Zeta Run to ensure measurement stability. Furthermore, the Zeta Potential analysis was performed at a controlled temperature of 25°C, with a refractive index set at 1.318 for a wavelength of 1550 nm, and a viscosity of 0.0091 poise (Lee and Ahn 2016).

3.3. Surface free energy analysis

Surface Free Energy (SFE) serves as a fundamental indicator of adhesion strength between materials and is commonly employed to assess the bonding efficacy within the binder-aggregate system (Guo *et al.* 2020, Khan *et al.* 2016b, Rudawska and Jacniacka 2018). It represents the energy required per unit area to expand the material surface and is denoted by the symbol γ (Kakar *et al.* 2016, Ziyani

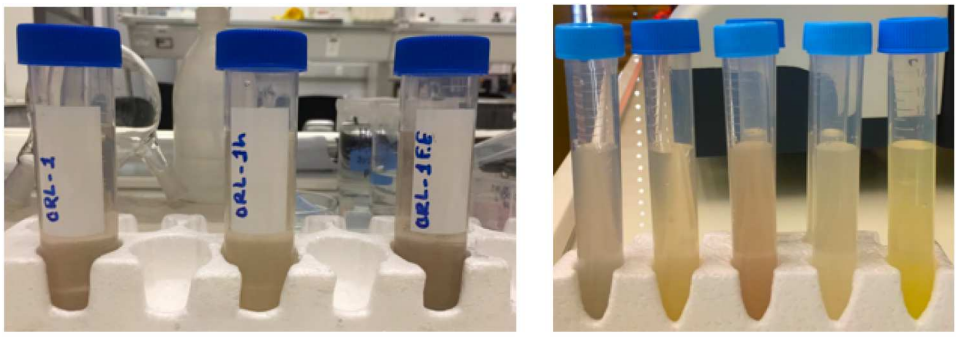

(a) (b)

Figure 2. AE and aggregates solutions for Zeta Potential tests. (a) Asphalt Emulsion solutions for Zeta Potential analysis and (b) Aggregates solutions for Zeta Potential analysis.

et al. 2016). SFE is typically measured in ergs/cm2 or mJ/m2. Young-Laplace formulated the basic equation (Equation 2) for determining SFE in solid materials based on the solid-liquid interface, which accounts for the contact angle (θ) formed as a result of the equilibrium of forces at the angle between the surface and the tangential contact of the drop γ_{SL} (Kakar *et al.* 2016, Rudawska and Jacniacka 2018, Schuster *et al.* 2018). This metric plays a critical role in understanding the interaction dynamics at solid-liquid interfaces, where surface tension phenomena occur, influencing the overall adhesion properties (Ziyani *et al.* 2016).

$$\gamma_{SL} = \gamma_{SV} - \gamma_{LV} \cdot \cos\theta \tag{2}$$

Likewise, the contact angle is analysed on an ideal solid surface, which refers to a chemically homogeneous and inert surface, perfectly smooth or low roughness, and within gravity or electromagnetism. So the contact angle does not vary throughout the solid-liquid interface contact line, for which it represents a solid surface local average (Schuster *et al.* 2018). Based on Equation (2), the Good-van Oss-Chaudhury (GVOC) method re-defined Equation (3) to determine the SFE in terms of dispersive and polar components.

$$\gamma = \gamma^{LW} + \gamma^{AB} = \gamma^{LW} + 2\sqrt{\gamma^{+}\gamma^{-}} \tag{3}$$

Dispersive and polar components are Lifshitz-Van der Waals and Lewis acid-base interactions, respectively. Lifshitz-Van der Waals interactions represent the non-polar component (London dispersive force) defined as γ^{LW} and Lewis acid-base interactions represent the polar component, which involves interactions of acceptor γ^{+} (acid component) and donor γ^{-} (base component) of electrons, defined as γ^{AB}. The Good-van Oss-Chaudhury (GVOC) method is also established as presented in Equation (4) representing the solid-liquid interface adhesion work (Kakar *et al.* 2016, Khan *et al.* 2016b, Rudawska and Jacniacka 2018). Moreover, adhesion work is understood as the energy needed to join two materials, or well, as the work required to separate two phases that are in equilibrium (Ebnesajjad 2011, Bahramian 2012). To evaluate the surface free energy (SFE) of a solid (asphalt, aggregate) indirect methods, such as contact angles, can be applied with the Sessile drop (GVOC theory) or Wilhelmy plate techniques (Kakar *et al.* 2016, Khan *et al.* 2016b). Thus, the SFE was determined by applying the Sessile drop method.

$$\begin{aligned} W_{LS}^{a} &= \gamma_L(1+\cos\theta) \\ &= 2\sqrt{\gamma_S^{LW}\gamma_L^{LW}} + 2\sqrt{\gamma_S^{+}\gamma_L^{-}} + 2\sqrt{\gamma_S^{-}\gamma_L^{+}} \end{aligned} \tag{4}$$

Initially, both aggregate and Residual Asphalt (RA) surfaces underwent meticulous preparation to ensure smoothness, cleanliness, and dryness before conducting contact angle measurements. The aggregate surfaces were obtained by sliding 5-inch rocks, while the Residual Asphalt (RA) surfaces were prepared under both cold and hot conditions. The Cold Residual Asphalt (CRA) state was achieved by immersing a glass sheet in the Asphalt Emulsion (AE), leading to the formation of a Residual Asphalt (RA) film upon the breakdown of the AE. This approach aimed to replicate conditions relevant to Cold Mix Asphalt (CMA) preparation and facilitate comparison with Residual Asphalt (RA) obtained through conventional methods.

The cold process, a new experiment in the laboratory, was a key fact for this investigation. On the first instance, Glass, with a negative charge, broke down the asphalt emulsion. Furthermore, measuring contact angles was relevant to simulate asphalt emulsion breaking when interacting with aggregate (without heat) in CMA manufacturing. The glass sheet was immersed in the asphalt emulsion from 3 up to 6 times to achieve a solid asphalt film based on the type of AE and surfaces were then dried for 24 h in a desiccator before contact angle testing. In fact, the cold process was not only innovative but also highly effective. The procedure was repeated many times to ensure consistent, reliable results, highlighting the meticulousness of the experimental setup.

Conversely, for the Hot Residual Asphalt (HRA) state, Residual Asphalt (RA) was derived from the AE through the evaporation test following ASTM D6934 standards. Subsequently, the glass sheet was immersed in the Hot Residual Asphalt (RA) to form the film. Both aggregate and Residual Asphalt (RA) surfaces were then placed in a desiccator for 24 h to ensure thorough drying and environmental protection. Contact angles were measured using an automated dispensing system integrated with the Ramé-Hart goniometer, which

Table 1. Basic characterisation and properties of aggregates under study.

Property	Coello River	Guayuriba River	Mondoñedo Quarry	Standard
Ten per cent fines (%) Dry; Wet	231; 196	272; 218	184; 121	BS 20290
Flat and elongated particles (%)	3.0	2.0	1.0	ASTM 4791
Absorption (%)	1.40	1.20	4.60	ASTM C127
Specific gravity	2.73	2.25	2.47	ASTM C127
Los Angeles Abrasion (%)	24.0	20.0	49.0	ASTM C131
pH	8.68	8.24	7.75	ASTM D4972

dispensed 10 l of water, formamide, and ethylene glycol Sessile drops onto the prepared surfaces for angle measurement.

4. Results and discussion

4.1. Basic characterisation of asphalt emulsion and aggregates

The basic characterisation of both Asphalt Emulsion (AE) and aggregates was conducted in accordance with the Colombian technical regulations, as outlined in Table 2. The results of this characterisation are presented in Table 3 for AE and Table 1 for aggregates. Additionally, the composition of AE was verified through Infrared Spectroscopy (IR) using an IRTracer-100, with tests conducted for both AE and their Residual Asphalt (RA) obtained under cold conditions. Similarly, the mineral composition of the aggregates was verified through X-Ray Diffraction (XRD) using an XRD-7000L equipment and X-Ray Fluorescence (XRF) using a XRF-1800 Shimadzu sequential spectrometer. These analyses provided crucial insights into the chemical composition and structural characteristics of both the AE and aggregates, essential for understanding their properties and behaviour in subsequent experimental tests.

4.2. Infrared spectroscopy of asphalt emulsions

Figure 3 depicts the IR analysis results for Asphalt Emulsion (AE) and Residual Asphalt (RA). The AE spectrum reveals prominent O-H bands at 3416 cm^{-1} and 1647 cm^{-1}, indicative of water content (Ge *et al.* 2020, Li *et al.* 2015, Zhang *et al.* 2020). Additionally, it exhibits C-H(CH3) bands at 2923 cm^{-1} and 1375 cm^{-1}, along with C-H(CH2) bands at 2850 cm^{-1} and 1458 cm^{-1}, corresponding to aliphatic groups (You *et al.* 2020). Moreover, the presence of C=C (1600 cm^{-1}) and C-H (742 cm^{-1}) bands signifies aromatic groups (You *et al.* 2020, Zhang *et al.* 2020). Notably, the intensity of small aliphatic group bands varies among the three AE types, with CSS-1h displaying the highest intensity, possibly indicating greater aliphatic group content. Furthermore, a strong peak observed in the spectrum between 2850 and 2923 cm^{-1} signifies the presence of abundant aliphatic C-H (carbon-hydrogen) bonds. These bonds are associated with the saturated and unsaturated hydrocarbon fractions of the asphalt binder, which are relevant components for the emulsion's performance (viscosity, waterproofing, and long-term durability), as suggested Camargo *et al.* (2020) and Mazalan *et al.* (2023).

This observation may stem from increased aliphatic group intensity in Cold Residual Asphalt (CRA) and Hot Residual Asphalt (HRA), suggesting slight AE breaking due to exposure to environmental conditions. Specifically, the O-H band at 3416 cm^{-1} is present in CRA, suggesting partial breaking, whereas it is absent in HRA. Additionally, the presence of S=O (1031 cm^{-1}) and C=O (1700 cm^{-1}) bands, corresponding to sulfoxides and carbonyl acid, respectively, is more pronounced in HRA due to the asphalt aging process at higher temperatures. These bands intensify with increased aging grade (Ge *et al.* 2020). Hence, by detecting these aliphatic C-H stretches through FTIR, we can gain valuable information about the asphalt emulsion's suitability.

Moreover, the observed variations are primarily linked to fluctuations in the dosage of the emulsifying agent utilised during emulsion preparation. On the other hand, these variations in C-H bond characteristics might correlate with observed discrepancies in zeta potential, a measure of surface charge. For instance, the CSS-1h emulsion exhibited a stronger C-H peak and a higher zeta potential value compared to other emulsions. However, it's crucial to acknowledge that factors beyond the chemical composition, such as particle size and environmental conditions, can also influence zeta potential measurements.

4.3. Mineralogical composition of aggregates

The mineralogical composition obtained through XRD/XRF analysis is depicted in Figure 4 for all three aggregates under study. Coello River (CR) aggregate displays a more diverse range of chemical compounds compared to Guayuriba River (GR) and Mondoñedo Quarry (MQ), particularly showcasing the presence of silicon dioxide (SiO_2), aluminum oxide (Al_2O_3), calcium oxide (CaO), iron (III) oxide (Fe_2O_3), and

Table 2. Colombian techcnical specifications fulfilment for Asphalt Emulsions tests.

\cmidrule(r){2-3}\cmidrule(l){4-5} Property	CSS-1 Min. Value	CSS-1 Max. Value	CSS-1h Min. Value	CSS-1h Max. Value
pH	–	5.0	–	5.0
Saybolt furol viscosity (s), @25 °C	20.0	200.0	20.0	100.0
Residual Asphalt (RA) (%)	57.0	–	57	–
Electric Charge of Particles[a]	Positive			

[a]Electric Charge of Asphalt Emulsion particles were corroborated with Zeta Potential tests.

Table 3. Basic characterisation and properties of Asphalt Emulsions under study.

Property	CSS-1	CSS-1 SF	CSS-1h	Standard
pH	2.44	2.29	2.56	EN 12850
Particle Sizer d_{10}	0.67	2.07	0.92	–
Particle Sizer d_{50}	4.94	8.69	2.65	–
Particle Sizer d_{90}	15.80	34.40	10.10	–
Saybolt furol viscosity (s), @25°C	32.0	27.0	39.7	ASTM D7496
Residual asphalt (%)	58.3	58.0	59.7	ASTM D6934
Density (g/cm^3), @25°C	0.90	0.91	0.88	ASTM D6937

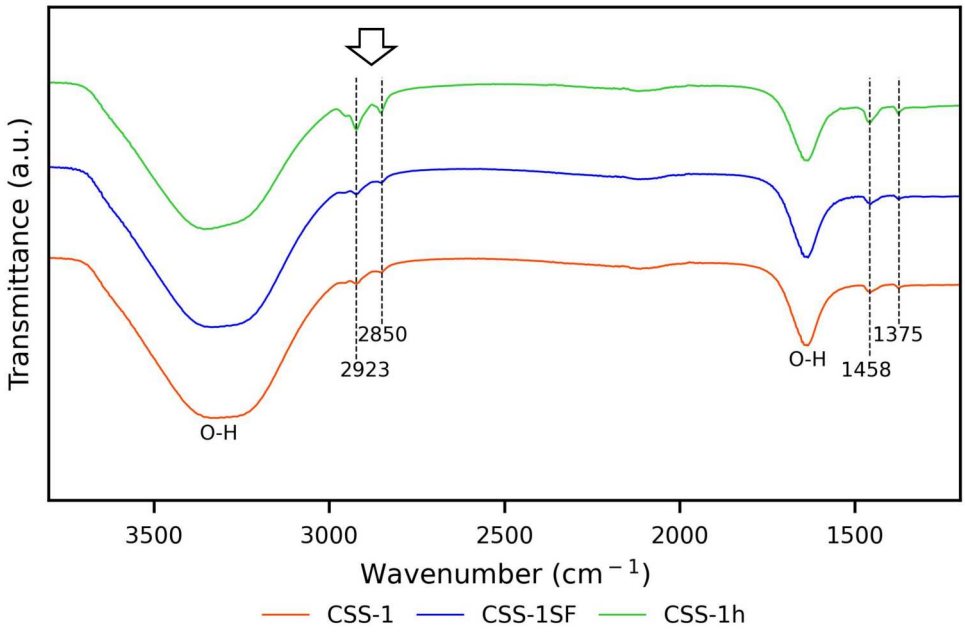

Figure 3. IR spectra of asphalt emulsions (AE) and Residual Asphalts (CRA and HRA).

potassium oxide (K_2O). This disparity could be attributed to MQ aggregate's higher homogeneity resulting from its geological facies and depositional conditions, unlike the alluvial aggregates (CR and GR) composed of a clastic mix originating from diverse locations along the river.

Furthermore, a correlation between the SiO_2 content and the aggregate pH was observed, suggesting that the aggregate with the highest SiO_2 content (84.84%) exhibits the lowest pH value (7.75), corresponding to MQ aggregate. Conversely, the aggregate with the lowest SiO_2 content (59.82%) demonstrates the highest pH value (8.68), attributed to CR aggregate. These SiO_2 content variations classify MQ and GR as acidic aggregates ($SiO_2 > 66\%$), while CR is categorised at an intermediate level (59.82%) (Gorman *et al.* 2004).

Acidic aggregates are hydrophilic materials that generate poor adhesion with asphalt as the asphalt film requires a hydrophobic surface as that of basic aggregates for better adhesion (Cala and Caro 2022, Gorman *et al.* 1998, Lee and Ahn 2016, Ziyani *et al.* 2014). Thus, as acidic aggregates are hydrophilic, prefer water to asphalt, which is the opposite of basic aggregates (Tang *et al.* 2021). Therefore, the bond of the asphalt-aggregate system is strongly promoted by basic aggregates (there is the formation of insoluble salts), and lightly promoted by acidic aggregates (there is the formation of soluble salts) due to they develop a repulsion force with the asphalt, but an attraction force with the water (Bagampadde 2005). Furthermore, Gorman *et al.* (2004) showed that SiO_2, Al, Na, and K increase the polarity of the aggregate surface, therefore, undermining the adhesion with asphalt. On the contrary, the presence of Mg, Ca, and Fe reduces aggregate polarity and improves adhesion.

Based on the findings, MQ aggregate exhibited the highest concentration of the polar element (SiO_2) and the lowest concentration of the non-polar element (Fe_2O_3), rendering it the most polar aggregate among the three (Bagampadde 2005). This underscores the significance of the Al_2O_3 and SiO_2 content, as demonstrated by Chew *et al.* (2020), who indicated that these elements reduce asphalt stiffness and enhance aggregate coating. Moreover, the presence of calcium oxide (CaO) contributes to the mastic's stiffness, thereby fortifying the bond between the binder and the aggregate. Additionally, as noted by Liu *et al.* (2016), CaO and MgO can undergo reactions with water, forming calcium and magnesium hydroxides, respectively, thereby enhancing the asphalt mix's resistance to moisture damage.

Given that Cationic Asphalt Emulsion (AE) needs to undergo breaking (separation of water and asphalt) upon interaction with the aggregate, acidic aggregates are conducive to facilitating this process due to their negative electrical charges, which generate an attractive force between them. Conversely, basic aggregates alter their positive charge to negative upon exposure to water, thereby promoting the breaking of cationic AE. Consequently, cationic AE is regarded as versatile for effectively interfacing with all aggregate types, making it the preferred choice for pavement construction (Gorman *et al.* 2004, Ronald and Luis 2016, Thanaya 2003).

Moreover, Wates and James (1993) and Gorman *et al.* (2004) showed that acidic aggregates are suitable for good adhesion with cationic asphalth emulsion (AE). However, basic aggregates undergo poor adhesion due to their neutral electric charge when mixed with cationic AE. In short, Coello River (CR), Guayuriba River (GR) and Mondoñedo Quarry (MQ) aggregates are mainly composed of SiO_2 and Al_2O_3 that make them polar and acidic. Thus, it is expected an attractive force with the three AE and a better electrochemical interaction with MQ aggregate since it presented a higher acidic condition and thus a higher reactive comportment to destabilise the AE.

4.4. Zeta potential of asphalt emulsions

The Zeta Potential (ZP) of Asphalt Emulsion (AE) under various pH conditions is depicted in Figure 5. Notably, CSS-1h consistently exhibits the highest ZP values across the entire

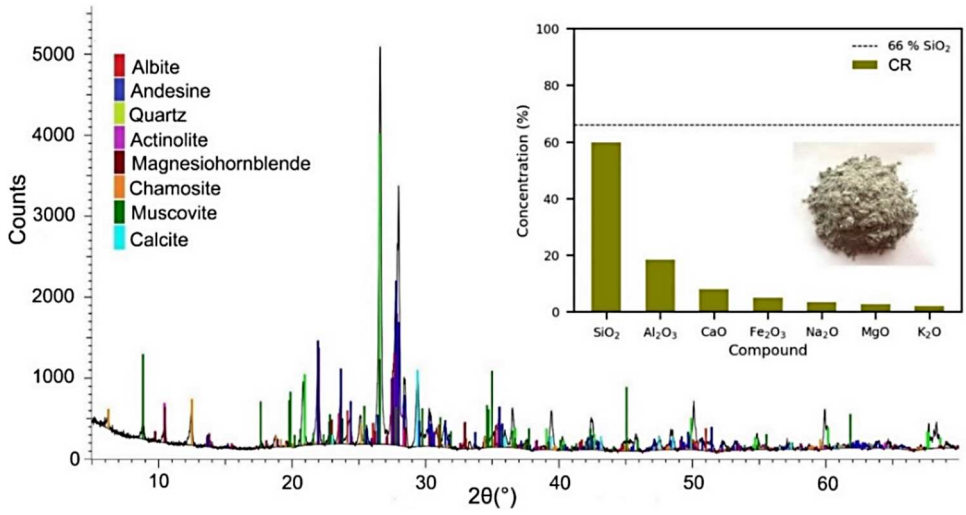

(a)

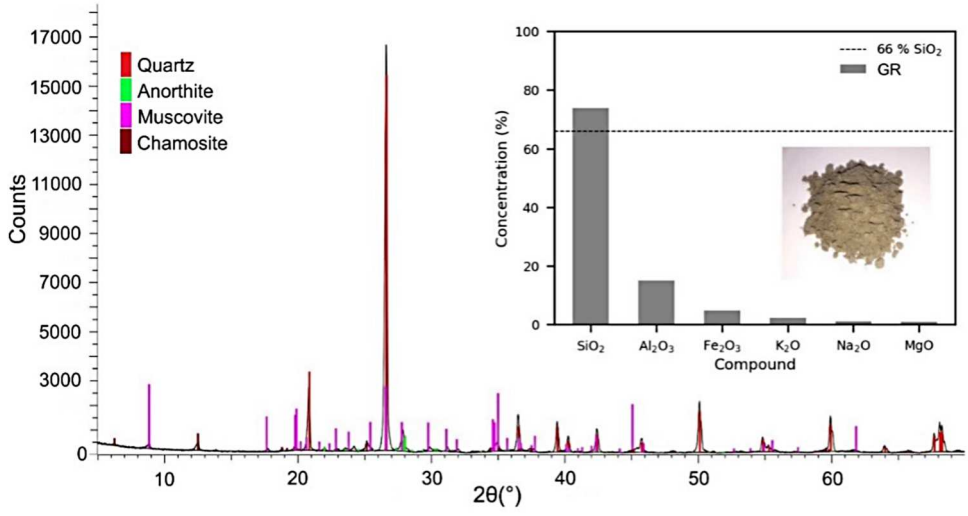

(b)

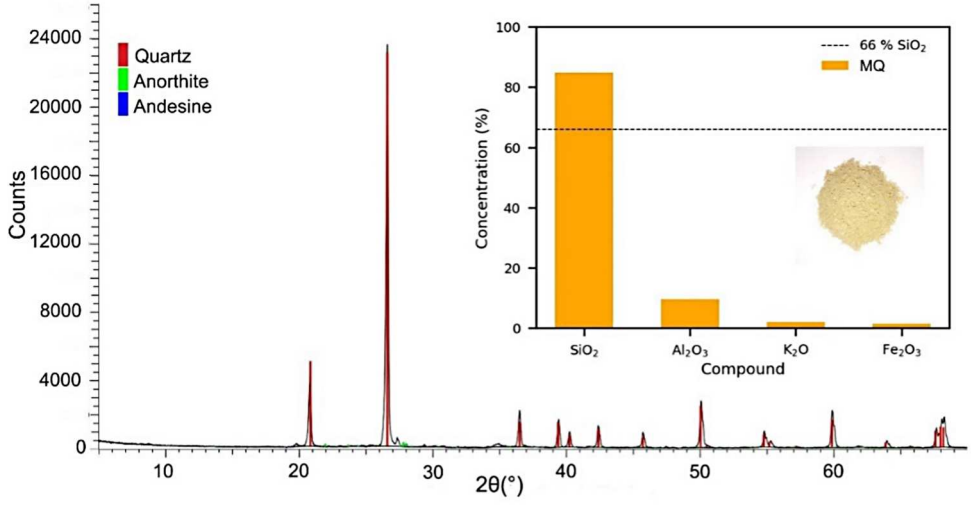

(c)

Figure 4. Mineralogical composition of aggregates under study through XRD and XRF analysis. (a) Mineralogical composition of CR aggregates. (b) Mineralogical composition of GR aggregates and (c) Mineralogical composition of MQ aggregates.

pH spectrum, while CSS-1 SF consistently displays the lowest ZP values. It's observed that CSS-1h maintains a positive ZP throughout all pH levels, whereas CSS-1 and CSS-1 SF exhibit negative ZP values at pH 5, 8, and 9. Additionally, the AE ZP peaks at pH 2.5, with CSS-1 and CSS-1 SF displaying similar behaviour across the pH range, unlike CSS-1h. Consequently, CSS-1 and CSS-1 SF ZP exhibit sensitivity within the pH range, transitioning from positive to negative charges, while AE ZP remains positive under equilibrium conditions at pH 7, as anticipated.

Several studies have investigated the relationship between zeta potential (ZP) and the stability of amphoteric emulsifiers (AEs). As reported by Cui and Pang (2017), a high ZP indicates good AE stability, particularly at lower pH ranges. This is because the formation of hydrochlorides by the emulsifier enhances both its solubility and emulsification capabilities. Furthermore, the research of Wates and James (1993) highlights the influence of pH on ZP in cationic AEs. In low pH environments, greater emulsifier ionisation leads to an increased ZP. Conversely, high pH conditions lead to a reduced ZP due to unfavourable emulsifier ionisation. This shift from positive to negative ZP in high pH environments occurs due to the deprotonation of the emulsifier's amine groups and asphalt ionisation.

This behaviour of the emulsifier is known as amphoteric, which leads to a lack of adhesion with the aggregates (Wates and James 1993). The above remains consistent as reported by Labib (1992), which highlighted that asphalt cement with an amphoteric nature is expected to develop a low adhesion interface with the aggregate when water is present, which generates its separation from the aggregate. Therefore, CSS-1h will develop a stable interaction with the three aggregates due to its permanent positive ZP in the entire pH range. Hence, due to the amphoteric nature, CSS-1 and CSS-1 SF will develop a low adhesion with the three aggregates. On the other hand, Wang *et al.* (2013) established that AE stability is favoured by a stable ZP or a slight increase in pH, causing a delay in the AE breaking during storage. Additionally, large ZP is associated with the AE rapid breaking during mixing (Wates and James 1993).

This study investigated the relationship between zeta potential (ZP) and particle size (d10, d50, and d_{90}) for anionic emulsions (AE) in asphalt emulsions, as suggested by Diaz-Romero and Braham (2022). Understanding these factors is crucial as they influence not only the rheological properties (flow behaviour) of the asphalt emulsion but also its overall stability. Our findings revealed that CSS-1 SF had the largest diameter (8.69 m) and the lowest ZP, followed by CSS-1. Conversely, CSS-1h exhibited the smallest diameter (2.65 m) and the highest, most stable ZP. Interestingly, the point of zero charge (PZC) wasn't observed for any of the three AEs. This suggests that the permanent positive ZP of CSS-1h prevented extreme deprotonation of the emulsifier, thereby inhibiting residual asphalt (RA) ionisation (which would lead to a negative ZP). In contrast, CSS-1 and CSS-1 SF likely experienced significant deprotonation, leading to RA ionisation and negative ZP values at high pH. However, these negative charges weren't fully neutralised.

Figure 5 illustrates the Zeta Potential (ZP) of aggregates under different pH conditions. It's noteworthy that the ZP remained negative across the entire pH spectrum, with the least negative values observed at pH 2 and 2.5, and the most negative values at pH 5, 7, 8, and 9. This phenomenon is attributed to the compression and expansion of the double layer, respectively (John and Arnepalli 2019). Therefore, it's plausible to infer that AE breaking in the presence of the aggregate is favourable when the interaction pH is up to 2.5, as the aggregate becomes more negatively charged, aiding in AE destabilisation. Furthermore, Figure 5 provides insight into the electric charge analysis of both the three asphalt emulsions and the three aggregates. This analysis aims to identify their attraction potential concerning pH variations at their interface. It's observed that under basic pH conditions (8 and 9), both materials exhibit negative ZP values, indicative of low electrochemical attraction due to charge affinities. Additionally, Figure 11 depicts the electrostatic interaction of the AE-aggregate system, derived from the independent evaluation of their electrical charges.

The observed zeta potential (ZP) behaviour of the asphalt emulsions (AEs) highlights the critical role of pH in their

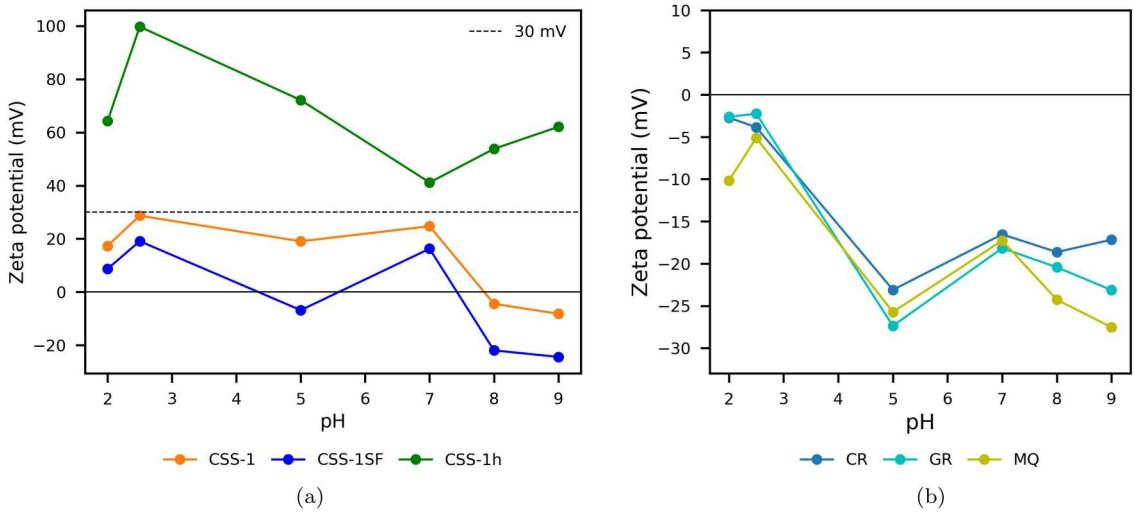

Figure 5. Zeta Potential of asphalt emulsions and aggregates under study. (a) Zeta Potential of asphalt emulsions and (b) Zeta Potential of aggregates.

stability and adhesion with aggregates. Around pH 2.5, the AEs exhibit a more positive ZP, making them less prone to breaking due to the low polarity of the aggregates at that pH. However, both CSS-1 and CSS-1 SF display a shift towards negative ZP at higher pH values (5, 8, and 9). Therefore, for optimal performance, achieving a pH between 2.5 and 5 during the mixing of AE and aggregate is desirable. This pH range promotes a favourable electrochemical interaction due to strong affinity between the acidic minerals in the aggregates and the cationic emulsifiers, leading to enhanced adhesion.

Conversely, mixing neutral or positively charged minerals with cationic AEs results in poor adhesion because similarly charged particles lack attractive forces. While Lee and Ahn (2016) reported stability for aggregates with negative ZP between pH 2 and 11, this study observed a decrease in ZP for CSS-1h at pH 8 and 9, transitioning to negative values for CSS-1 and CSS-1 SF. This shift indicates potential chemical changes within the system at higher pH. Furthermore, the observed emulsion breakdown across all prepared solutions, evident from the dispersion of fine asphalt particles, underscores the dynamic nature of emulsion stability under varying pH conditions. Interestingly, though increasing the pH could theoretically make the emulsions resemble anionic emulsions, our focus was on observing the performance of each emulsion regarding stability variations related to protonation resulting from formulation differences (emulsifier dosage). In this context, the CSS-1h emulsion exhibited fewer ZP changes compared to the others (Figure 5). This could be attributed to changes in the dispersed phase and solubility affected by protonation due to a higher level of emulsifier.

In addition, dissolution processes refer to the surface groups ionisation of the aggregate, which develops positive or negative electrical charge. Acidic surface groups ionise with a negative electrical charge and basic surface groups with a positive electrical charge. Moreover, when AE and aggregate particles are in an ionic medium, polar ions are attracted to their surfaces. Thus, AE and aggregate particles acquire positive or negative electrical charges depending on the sign of the attracted ion (Thanaya 2003) as an ion adsorption process. According to He *et al.* (2022), PZC was not identified with the three aggregates possibly due to the high content of SiO_2, which has a negative charge and avoids neutralising the charge with the H^+ ions in low pH, however, ZP was less negative for the three aggregates.

The analysis of zeta potential in the context of asphalt emulsions and aggregates elucidate several aspects. Firstly, the variation in zeta potential with pH offers valuable insights into the stability and interaction dynamics of these systems. The observed ZP values for different emulsions (CSS-1h, CSS-1, and CSS-1 SF) reveal distinct electrochemical characteristics. Notably, CSS-1h exhibits a consistently positive ZP, suggesting superior stability throughout the pH range compared to CSS-1 and CSS-1 SF, which lose their positive charge at certain pH levels. Hence, the observed correlation between zeta potential (ZP) and emulsion stability, substantiated by prior research, underscores the critical importance of determining the optimal pH range during mixing. This targeted pH management strategy ensures optimal adhesion between emulsions and aggregates. Likewise, the dynamic changes in ZP highlight the importance of considering formulation variations and emulsifier dosages to achieve the desired performance characteristics in asphalt emulsions, the stability, and adhesion.

On the other hand, SiO_2 and Al_2O_3 are common components in all three aggregates. Therefore, the Zeta Potential (ZP) under basic or natural pH conditions was correlated with the SiO_2/Al_2O_3 ratio. Figure 6 illustrates the change in ZP ($\delta\zeta$) from pH 2 to 8, showing that GR exhibits the largest $\delta\zeta$, while MQ shows the largest change from pH 7 to 9. Although the $\delta\zeta$ is not distinctly clear from pH 2 to 8 for all three aggregates, a clear trend emerges from pH 7 to 9. Furthermore, the $\delta\zeta$ from pH 7 to 9 was modelled against the SiO_2/Al_2O_3 ratio using a logarithmic model (Figure 6(b)), yielding an R^2 coefficient of 0.99. This indicates that the higher ZP observed in MQ is attributed to its higher SiO_2/Al_2O_3 ratio, while the lower ZP in CR is associated with its lower SiO_2/Al_2O_3 ratio. Hence, the ZP of both AE and aggregates emerges as a crucial parameter influencing their interaction. A highly charged AE fosters a strong attractive force with the aggregate, facilitating rapid breaking (Needham 1996). However, it's important to note that AE pH reduction affects

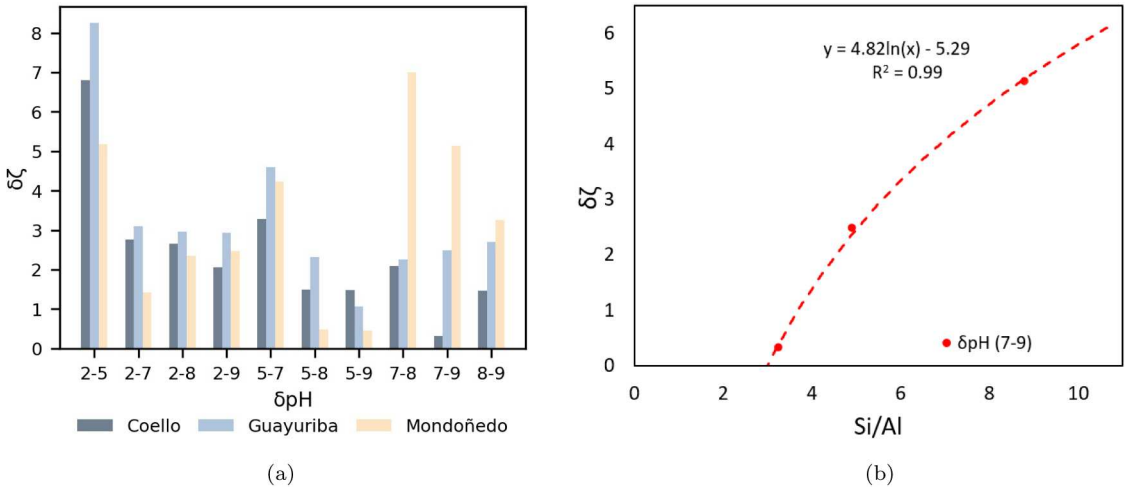

Figure 6. Changes in Zeta Potential ($\delta\zeta$) with pH change (δpH). (a) Zeta Potential change ($\delta\zeta$) with pH change (δpH) and (b) Zeta Potential with Si/Al ratio.

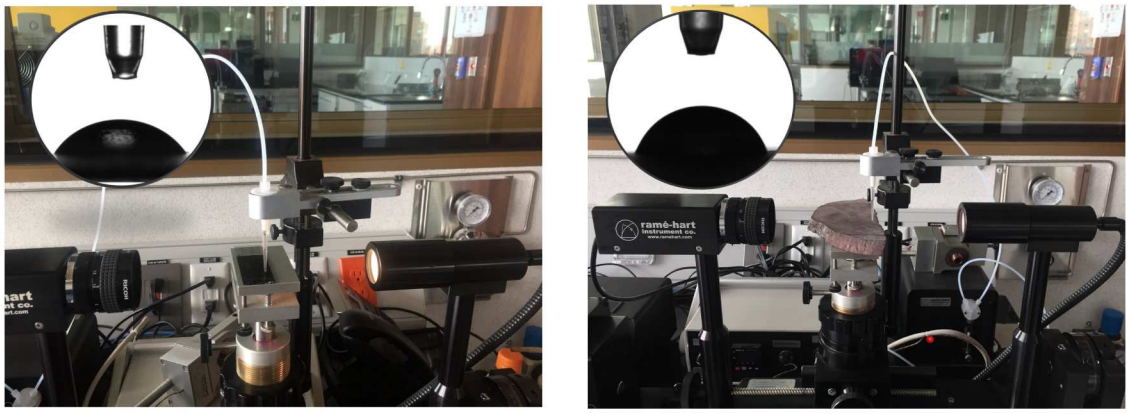

Figure 7. Contact angle for CRA and HRA Residual Asphalts under study. (a) Contact angle of CRA Residual Asphalt and (b) Contact angle of HRA Residual Asphalt.

the ZP of aggregates, thereby influencing the degree of interaction.

4.5. Surface free energy tests

Initially, the assessment of surface free energy focussed solely on the asphalt residue. This choice was driven by the requirement of the sessile drop method for a smooth and dry surface to ensure accurate measurement. The primary objective was to obtain a quantitative parameter for each material's surface free energy and subsequently analyse their interaction comprehensively. However, it's important to note that due to the testing conditions of the sessile drop method, evaluating the interaction during the coalescence stage, when the Asphalt Emulsion (AE) remains in a liquid state, posed significant challenges. Despite attempts, this aspect proved to be a complex process to address.

Hence, the contact angles of Cold Residual Asphalt (CRA) and Hot Residual Asphalt (HRA) are presented in Figure 7. It is observed that CRA contact angles are lower than those from HRA, and most of the contact angles formed with water are less than 90°, except for the HRA CSS-1h-water system (92.86°) as showed in Figure 8. This suggests that most Residual Asphalt (RA) samples are hydrophilic (Wu *et al.* 2020, Ziyani *et al.* 2016), with HRA CSS-1h being the most hydrophobic. However, HRA is less hydrophilic than CRA. In general, low contact angles are associated with a high wetting surface (Ziyani *et al.* 2016). Surface Free Energy (SFE) with its components for Residual Asphalt (RA) are indicated in Figure 9. Moreover, it is observed that CRA SFE is higher than that of HRA, which is consistent with the contact angle results. Even so, the CRA and HRA SFE follow an ascending order of CSS-1 < CSS-1 SF < CSS-1h, with non-polar components being higher representatives except for CSS-1 HRA.

As noted by Latifi and Amini (2020), high values of non-polar components indicate low polarity for the asphalt. Conversely, high Surface Free Energy (SFE) values indicate high polarity (Wu *et al.* 2020). Consequently, Cold Residual Asphalt (CRA), with the highest SFE values, is more polar, while Hot Residual Asphalt (HRA) loses that polarity when exposed to temperature. The SFE values for HRA closely

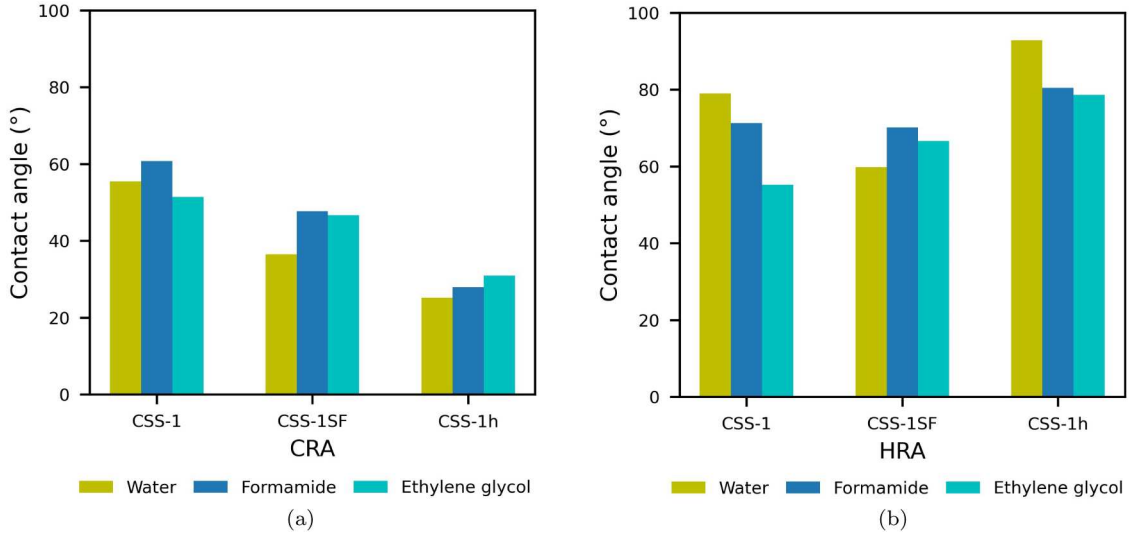

Figure 8. Contact angles in tests with residual asphalt and aggregates under study. (a) Contact angle test of Residual Asphalt and (b) Contact angle test of aggregates.

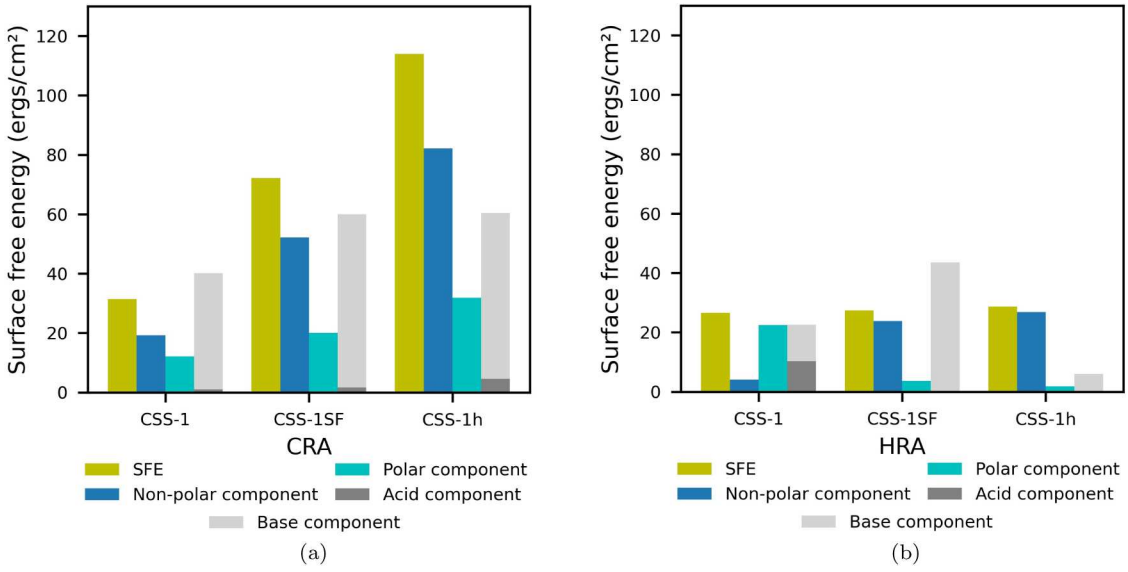

Figure 9. Surface Free Energy for CRA and HRA Residual Asphalts under study. (a) Surface Free Energy of CRA Residual Asphalt and (b) Surface Free Energy of HRA Residual Asphalt.

match those reported for asphalts in previous studies (Guo *et al.* 2014, Howson *et al.* 2011, Kakar *et al.* 2016, Wei and Zhang 2012), which fall within the range of 12.95 mJ/mm^2 to 35.78 mJ/m^2 and exhibit the highest non-polar component.

Figure 10 illustrates that all contact angles are below 90°, indicating a hydrophilic character (Wu *et al.* 2020, Ziyani *et al.* 2016). Furthermore, the contact angles of MQ aggregate with formamide and ethylene glycol are the lowest, and the contact angles formed with all three aggregates and ethylene glycol are generally the smallest. Additionally, MQ aggregate exhibits the highest Surface Free Energy (SFE) value, followed by CR and GR aggregates. Hence, the SFE of MQ can be compared with that of quartzite, considering its high SiO_2 content, as demonstrated in the study by Ziyani *et al.* (2016), where quartzite exhibits the highest surface free energy (SFE).

The composition of components emerges as a key factor shaping interaction dynamics. Notably, the balance between non-polar and polar components delineates the Surface Free Energy (SFE) of Coello River (CR), Guayuriba River (GR) and Mondoñedo Quarry (MQ) aggregates. A preponderance of polar components in an aggregate implies a stronger affinity for water, potentially compromising bonding with asphalt in moist conditions, as suggested by Khan *et al.* (2016a). Conversely, asphalt, with a lower polar component compared to the aggregate, requires increased polarity to enhance compatibility and bonding strength, a point emphasised by Tanzadeh and Shafabakhsh (2020).

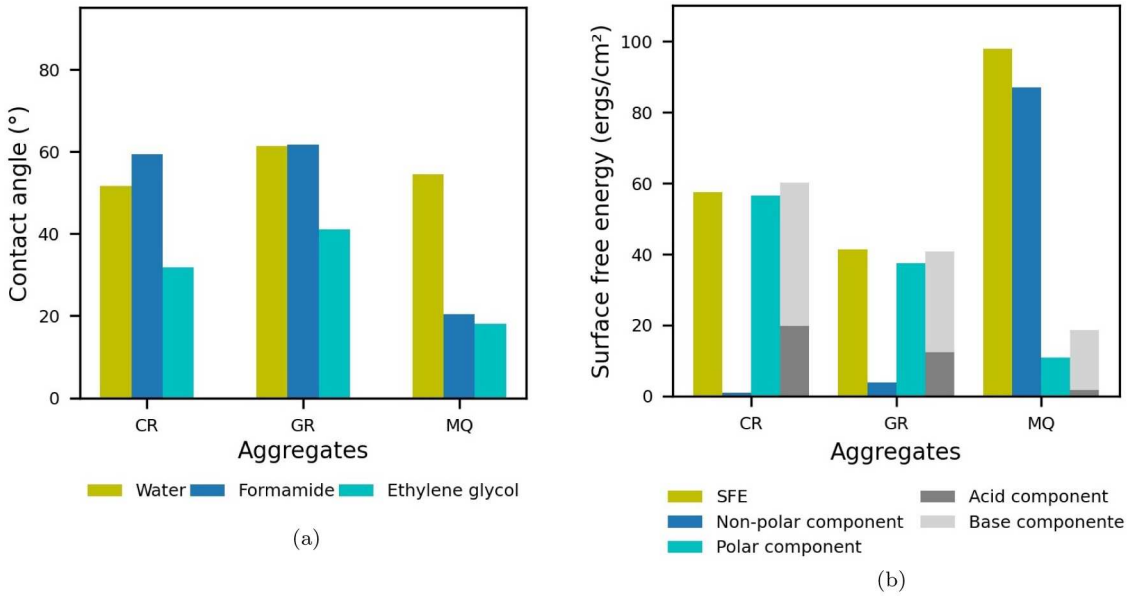

Figure 10. Contact Angle and Surface Free Energy for aggregates under study. (a) Contact Angle of aggregates and (b) Surface Free Energy of aggregates.

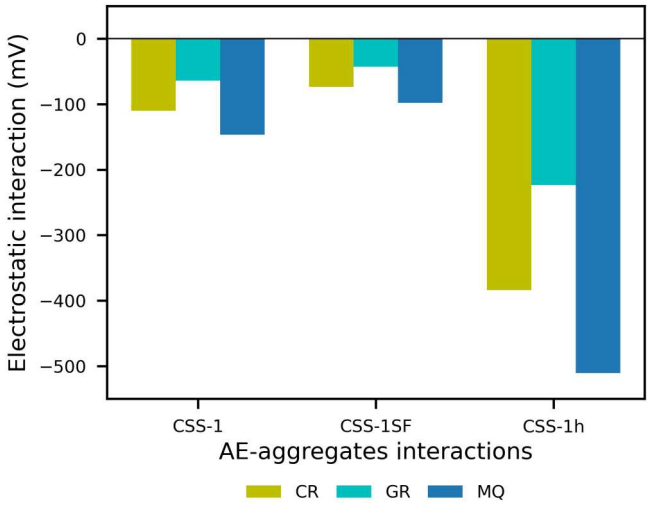

Figure 11. Asphalt emulsions and aggregates interactions.

In the case of Cold Residual Asphalt (CRA) and Hot Residual Asphalt (HRA), their polar components are overshadowed by those of the aggregates. However, CRA demonstrates a notable propensity for interaction with aggregates, as noted by Latifi and Amini (2020). The correlation between higher SFE values and stronger bonds, as elucidated by Latifi and Amini (2020), suggests the likelihood of robust bond formation between aggregates and CRA due to their elevated SFE values and greater polarity compared to HRA, as discussed by Wu *et al.* (2020).

A critical aspect of optimising mixture performance lies in comprehending the relationship between the surface chemistry of the aggregate and its adhesion to asphalt. Figure 10 exemplifies this concept by establishing a correlation between the Surface Free Energy (SFE) and contact angles of three distinct aggregates, and their potential for adhesion to the asphalt residue remaining from the studied emulsions. Notably, the Mondoñedo aggregate exhibits the highest SFE, and the lowest contact angles, relating it to a higher adhesion potential with the residual asphalt. Figure 11 serves to complement this analysis by directly evaluating the attractive forces between each emulsion and aggregate using zeta potential. Furthermore, the Mondoñedo aggregate consistently exhibits the strongest attractive forces, thereby associate its potential to destabilise the asphalt emulsions. Hence, these findings underscore the critical importance of considering both the inherent properties of the aggregate (SFE) and its interaction with the emulsion (zeta potential) when selecting materials to ensure optimal mixture performance.

4.6. Electrochemical interaction of the asphalt emulsion-aggregate system

Figure 11 illustrates the interaction between AE and aggregates based on the ZP results. Previous studies (Lee and Ahn 2016, Labib 1992) proposed multiplying the ZP of AE and aggregates at pH 2.5 to assess their interaction. The electrostatic interaction results were negative, indicating attractive forces between three AE and three aggregates (Lee and Ahn 2016). Notably, CSS-1h demonstrated the strongest attraction with aggregates, whereas CSS-1 SF showed the weakest. Among aggregates, Mondoñedo Quarry (MQ) exhibited the strongest attraction with AE, while Guayuriva River (GR) the weakest. This aligns with MQ's acidic nature, which enhances its affinity to cationic AE (Gorman *et al.* 2004, Wates and James 1993).

Generally, electrochemical interaction results correlate with the highest and lowest ZP values at pH 2.5 in the order of MQ > CR > GR and CSS-1h > CSS-1 > CSS-1 SF. Thus, higher positive and negative ZP values lead to stronger attractions for AEA-S compared to lower ZP values. Overall, superior performance is anticipated for CMA with CSS-1h and the three aggregates, particularly with MQ, compared to CSS-1 SF and the three aggregates, primarily with GR. It is relevant to highlight, the efficacy of interactions is represented by the tallest bars in the graph, corresponding to higher values of zeta potential and surface free energy (SFE) observed for both AE/RA and aggregates. This suggests more favourable bonding between the components. Consequently, CSS-1h emulsion and Mondoñedo aggregate exhibited the most promising interactions, implying potential for improved mechanical performance in the mixture.

On the other hand, Figure 12 illustrates interaction results between Residual Asphalt (RA) and aggregates according to the SFE results. In the first instance, all the adhesion work values are positive which means that the Residual Asphalt (RA) and aggregates have adhesion potential (Wei and Zhang 2012). Moreover, CRA presents greater adhesion work with the three aggregates than HRA which is associated with greater bond strength (Wei and Zhang 2012, Wu *et al.* 2020). The above is related to the highest SFE values for the CRA and aggregates with an ascending order of CSS-1 < CSS-1 SF < CSS-1h and GR < CR < MQ, which in fact, agrees with the adhesion work order as the highest SFE values lead to the greatest adhesion work (Guo *et al.* 2014, Wei and Zhang 2012). However, the HRA and aggregates adhesion works did not agree with the ascending order of their SFE (CSS-1 < CSS-1 SF < CSS-1h and GR < CR < MQ). The above lies with the calculation of the adhesion work since it is a function of the SFE components (non-polar, acid, and base components) and not directly of the total SFE.

5. Conclusions

In light of the research findings, a compelling conclusion emerges regarding the behaviour of asphalt emulsions. The Zeta Potential values, intricately tied to particle size (d_{10}, d_{50}, and d_{90}), as these factors not only influences the rheological properties of asphalt emulsion but also drives stability. Notably, asphalt emulsions characterised by smaller diameters exhibit remarkable stability (CSS-1h), whereas their larger-diameter counterparts (CSS-1 SF) demonstrate notably lower stability. This dichotomy arises from the potent repulsive forces generated by the small-diameter asphalt particles, overpowering the weaker forces within the larger-diameter particles.

Furthermore, a captivating revelation unfolds concerning the Zeta Potential of the three Colombian aggregates. These aggregates consistently manifest strong negative values across the entire pH spectrum, a phenomenon attributed to the dominant presence of SiO_2 and its intricate correlation with the

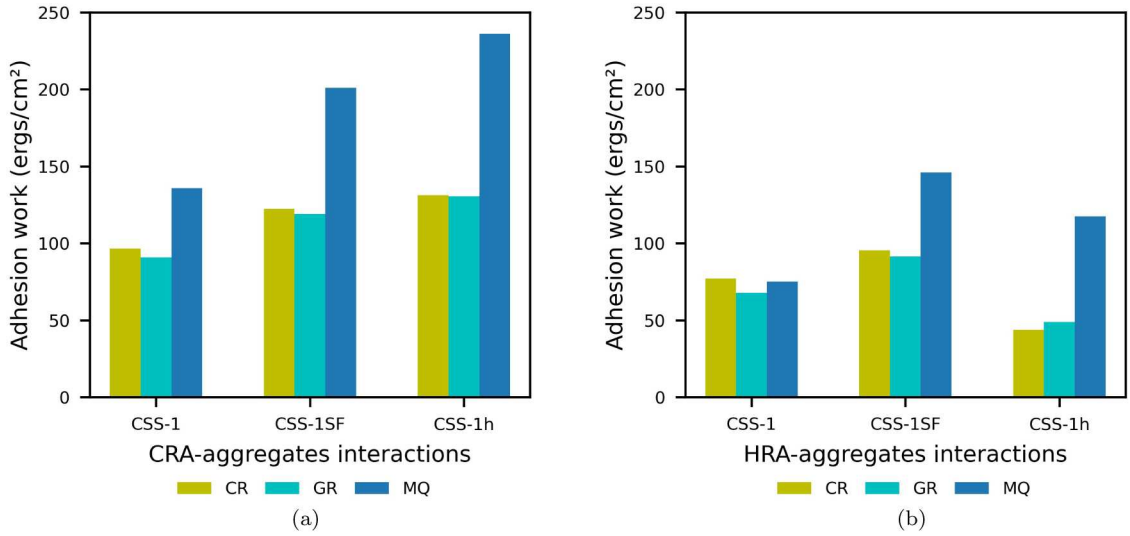

Figure 12. Residual Asphalts and aggregates interactions. (a) CRA and (b) HRA.

SiO_2/Al_2O_3 ratio. Particularly noteworthy is the quarry aggregate (MQ), which boasts the highest Zeta Potential, while the alluvial aggregates (CR and GR) exhibit comparably lower Zeta Potential values. This divergence stems from the significant homogeneity characteristic of the quarry aggregate's facie and depositional conditions, juxtaposed with the more varied nature of the alluvial aggregates.

By employing XRD and XRF analysis, we successfully uncovered a range of chemical compounds within the alluvial aggregates, including silicon dioxide (SiO_2), aluminum oxide (Al_2O_3), calcium oxide (CaO), iron (III) oxide (Fe_2O_3), and potassium oxide (K_2O). In contrast, the quarry aggregate exhibited a more limited composition. These findings have significant implications for performance disparities, with the quarry aggregate displaying higher polarity compared to the alluvial aggregates. This heightened polarity led to pronounced electrochemical interactions within the Asphalt Emulsion-Aggregate system (AEA-S). At the micro-scale, the AEA-S system demonstrated higher robust electrochemical interaction through elevated Zeta Potential and Surface Free Energy values. As we delve deeper into the implications, it becomes evident that the CSS-1h-MQ system holds the promise of outperforming CMA applications. This underscores the role of accurate aggregate chemical identification in establishing an electrochemical affinity within the AEA-S system. As we move forward, a nuanced understanding of these interactions stands to enhance the overall performance of the system and open avenues for innovation and improvement.

Acknowledgments

The authors would like to give a special thanks to MPI Ltda for providing asphalt emulsions during the whole investigation. Likewise, all authors contributed to the study conception, design, analysis, and manuscript writing. All authors read and approved the final manuscript. The data that support the findings of this study are available from the author, M.C.-B., upon reasonable request.

Disclosure statement

No potential conflict of interest was reported by the author(s).

Funding

The first author acknowledges the 'Vicerrectoría de Investigación' from the Pontificia Universidad Javeriana and CEIBA Foundation (Nariño) for the financial support received.

References

Alvarez, A.E., *et al.*, 2019. Adhesion quality of chip seals: comparing and correlating the plate-stripping test, boiling-water test, and energy parameters from surface free energy. *Journal of Materials in Civil Engineering*, 31 (3), 04018401-1–04018401-11. https://doi.org/10.1061/(ASCE)MT.1943-5533.0002603.

Bagampadde, U., 2005. *On investigation of stripping propensity of bituminous mixtures*. Thesis (PhD). KTH Royal Institute of Technology.

Bahramian, A., 2012. *Evaluating surface energy components of asphalt binders using wilhelmy plate and sessile drop techniques*. Thesis (PhD). Royal Institute of Technology (KTH).

Boulangé, L., Bonin, E., and Saubot, M., 2013. Physicochemical characterisations of the bitumen–aggregate interface to get a better understanding of stripping phenomena. *Road Materials and Pavement Design*, 14 (2), 384–403.

Cala, A., and Caro, S., 2022. Predictive quantitative model for assessing the asphalt-aggregate adhesion quality based on aggregate chemistry. *Road Materials and Pavement Design*, 23 (7), 1523–1543.

Camargo, I.G.D.N., *et al.*, 2020. Effect of thermal and oxidative aging on asphalt binders rheology and chemical composition. *Materials*, 13, 1–21.

Cardone, F., Virgili, A., and Graziani, A., 2018. Evaluation of bonding between reclaimed asphalt aggregate and bitumen emulsion composites. *Construction and Building Materials*, 184, 565–574.

Casillas, S., and Braham, A.F., 2022. Development of a performance-based approach to asphalt emulsion selection for cold in-place recycling applications. *Transportation Research Record: Journal of the Transportation Research Board*, 2676 (5), 104–115.

Castilla-Barbosa, M., Rincón-Arango, O., and Ocampo-Terreros, M., 2023. Electrokinetic forces as an electrical measure of chemical aging potential in granular materials. *ChemEngineering*, 7 (5), 91. https://doi.org/10.3390/chemengineering7050091.

Chew, J.W., *et al.*, 2020. Microscopic analysis and mechanical properties of recycled paper mill sludge modified asphalt mixture using granite and limestone aggregates. *Construction and Building Materials*, 243, 118172.

Cui, D., and Pang, J., 2017. The effect of ph on the properties of a cationic bitumen emulsifier. *Tenside Surfactants Detergents*, 54 (5), 386–392.

Dash, S.S., Chandrappa, A.K., and Sahoo, U.C., 2022. Design and performance of cold mix asphalt – a review. *Construction and Building Materials*, 315, 125687.

Day, D., Lancaster, I.M., and McKay, D., 2019. Emulsion cold mix asphalt in the uk: A decade of site and laboratory experience. *Journal of Traffic and Transportation Engineering (English Edition)*, 6 (4), 359–365.

Diaz-Romero, P.L., and Braham, A.F., 2022. Refining particle size specification for asphalt emulsion. *Construction and Building Materials*, 350, 128812.

Doyle, T.A., *et al.*, 2013. Developing maturity methods for the assessment of cold-mix bituminous materials. *Construction and Building Materials*, 38, 524–529.

Du, L., *et al.*, 2023. Upgrade of low rank coal by using emulsified asphalt and its application for preparation of coal water slurry with high concentration. *Journal of Dispersion Science and Technology*, 44 (6), 901–910.

Dukhin, A.S., and Xu, R., 2020. Zeta-potential measurements. In: V.-D. Hodoroaba, W.E.S. Unger, and A.G. Shard, eds. *Characterization of nanoparticles*. Amsterdam, Netherlands: Elsevier, 213–224. https://doi.org/10.1016/B978-0-12-814182-3.00014-6.

Ebnesajjad, S., 2011. Surface tension and its measurement. In: S. Ebnesajjad, ed. *Handbook of adhesives and surface preparation*. Kidlington, Oxford: Elsevier, 21–30.

Ge, D., *et al.*, 2020. Laboratory evaluation of the residue of rubber-modified emulsified asphalt. *Sustainability*, 12 (20), 8383.

Gorman, J.L., *et al.*, 1998. The role of aggregate surface chemistry in bitumen emulsion–aggregate interactions. *Road & Transport Research*, 7, 3. Available from: https://www.proquest.com/scholarly-journals/role-aggregate-surface-chemistry-bitumen-emulsion/docview/215250048/se-2?accountid=45660.

Gorman, J.L., Crawford, R.J., and Harding, I.H., 2004. Bitumen emulsions in road construction – a review. *Road & Transport Research*, 13, 25–38. Available from: https://www.proquest.com/scholarly-journals/bitumen-emulsions-road-construction-review/docview/215247083/se-2?accountid=45660.

Graziani, A., Virgili, A., and Cardone, F., 2018. Testing the bond strength between cold bitumen emulsion composites and aggregate substrate. *Materials and Structures*, 51 (1), 14. https://doi.org/10.1617/s11527-018-1139-6.

Guo, M., *et al.*, 2018. A state-of-the-art review on interfacial behavior between asphalt binder and mineral aggregate. *Frontiers of Structural and Civil Engineering*, 12 (2), 248–259.

Guo, F., *et al.*, 2020. Study on the adhesion property between asphalt binder and aggregate: A state-of-the-art review. *Construction and Building Materials*, 256, 119474.

Guo, M., Tan, Y., and Zhou, S., 2014. Multiscale test research on interfacial adhesion property of cold mix asphalt. *Construction and Building Materials*, 68, 769–776.

Han, S., Yao, T., and Yang, X., 2019. Preparation and anti-icing properties of a hydrophobic emulsified asphalt coating. *Construction and Building Materials*, 220, 214–227.

He, Y., *et al.*, 2022. Surface properties of eggshell powder and its influence on cement hydration. *Materials*, 15 (21), 7633.

Howson, J., *et al.*, 2011. Comprehensive analysis of surface free energy of asphalts and aggregates and the effects of changes in ph. *Construction and Building Materials*, 25 (5), 2554–2564.

Jain, S., and Singh, B., 2021. Cold mix asphalt: an overview. *Journal of Cleaner Production*, 280, 124378.

John, K.N., and Arnepalli, D.N., 2019. Factors influencing zeta potential of clayey soils. *In*: V.K. Stalin and M. Muttharam, eds. *Geotechnical characterisation and geoenvironmental engineering*. Singapore: Springer, vol. 16. https://doi.org/10.1007/978-981-13-0899-4.

Júnior, J.L.L., Babadopulos, L.F., and Soares, J.B., 2019. Aggregate–binder adhesiveness assessment and investigation of the influence of morphological and physico-chemical properties of mineral aggregates. *Road Materials and Pavement Design*, 20 (sup1), S79–S94.

Kakar, M.R., *et al.*, 2016. Surface free energy and moisture susceptibility evaluation of asphalt binders modified with surfactant-based chemical additive. *Journal of Cleaner Production*, 112, 2342–2353.

Khan, A., Redelius, P., and Kringos, N., 2016a. Evaluation of adhesive properties of mineral-bitumen interfaces in cold asphalt mixtures. *Construction and Building Materials*, 125, 1005–1021.

Khan, A., Redelius, P., and Kringos, N., 2016b. Toward a new experimental method for measuring coalescence in bitumen emulsions: A study of two bitumen droplets. *Colloids and Surfaces A: Physicochemical and Engineering Aspects*, 494, 228–240.

Labib, M., 1992. Asphalt-aggregate interactions and mechanisms for water stripping. *In*: *Abstracts of papers of the American chemical society, Amer Chemical Soc 1155 16th st, NW, Washington, DC 20036*. vol. 204, 68–FUEL.

Lastra-González, P., *et al.*, 2019. Mechanical assessment of the induction heating as a method to accelerate the drying process of cold porous asphalt mixtures. *Construction and Building Materials*, 208, 646–650.

Latifi, H., and Amini, N., 2020. Effect of aggregate type on moisture susceptibility of modified cold recycled mix asphalt: evaluation by mechanical tests and surface free energy method. *Frattura ed Integrità Strutturale*, 14 (52), 211–229.

Lee, J., and Ahn, H., 2016. Effect of electrical surface charge on seal coat curing and aggregate loss performance. *Journal of Testing and Evaluation*, 44, 20140318.

Li, N., *et al.*, 2015. Synthesis of a novel cationic asphalt emulsifier and its investigation by online ftir spectrophotometry. *Research on Chemical Intermediates*, 41 (4), 1935–1950.

Ling, C., Hanz, A. and Bahia, H., 2016. Measuring moisture susceptibility of Cold Mix Asphalt with a modified boiling test based on digital imaging. *Construction and Building Materials*, 105, 391–399. https://doi.org/10.1016/j.conbuildmat.2015.12.093.

Liu, X., *et al.*, 2016. Influence of moisture in aggregates on properties of cold-mixed resin asphalt mixture. *Construction and Building Materials*, 120, 232–240.

Liu, Y., *et al.*, 2020. Laboratory evaluation of emulsified asphalt reinforced with glass fiber treated with different methods. *Journal of Cleaner Production*, 274, 123116.

Malvern, I., 2015. *Zeta potential – an introduction in 30 minutes*. Malvern Instruments Limited.

Mazalan, N.A.A., *et al.*, 2023. Rheological properties of asphaltene-modified asphalt binder and mastic. *Physics and Chemistry of the Earth*, 131, 103422. https://doi.org/10.1016/j.pce.2023.103422.

Meng, Y., Ouyang, J., and Ou, J., 2023. Investigation on the wetting behavior of asphalt emulsion on aggregate for asphalt emulsion mixture. *Construction and Building Materials*, 400, 132844.

Miller, C., *et al.*, 2012. Surface energy characteristics and impact of natural minerals on aggregate–bitumen bond strengths and asphalt mixture durability. *Transportation Research Record: Journal of the Transportation Research Board*, 2267 (1), 45–55.

Needham, D., 1996. *Developments in bitumen emulsion mixtures for roads*. Thesis (PhD). University of Nottingham.

Pinto, I., and Buss, A., 2020. ζ potential as a measure of asphalt emulsion stability. *Energy & Fuels*, 34 (2), 2143–2151.

Ronald, M., and Luis, F.P., 2016. Asphalt emulsions formulation: state-of-the-art and dependency of formulation on emulsions properties. *Construction and Building Materials*, 123, 162–173.

Rudawska, A., and Jacniacka, E., 2018. Evaluating uncertainty of surface free energy measurement by the van oss-chaudhury-good method. *International Journal of Adhesion and Adhesives*, 82, 139–145.

Saadoon, T., Garcia, A., and Gómez-Meijide, B., 2017. Dynamics of water evaporation in cold asphalt mixtures. *Materials & Design*, 134, 196–206.

Salopek, B., Krasic, D., and Filipovic, S., 1992. Measurement and application of zeta-potential. *Rudarsko Geolosko Naftni Zbornik*, 4, 147–151.

Schuster, J.M., Schvezov, C.E., and Rosenberger, M.R., 2018. Construction and calibration of a goniometer to measure contact angles and calculate the surface free energy in solids with uncertainty analysis. *International Journal of Adhesion and Adhesives*, 87, 205–215.

Shanbara, H.K., *et al.*, 2021. The future of eco-friendly cold mix asphalt. *Renewable and Sustainable Energy Reviews*, 149, 111318.

Tan, W., *et al.*, 2022. Influence of aggregate chemical composition on the demulsification rate of emulsified asphalt. *Frontiers in Materials*, 9, 1079431. https://doi.org/10.3389/fmats.2022.1079431.

Tang, F., *et al.*, 2018. Study on the effect of demulsification speed of emulsified asphalt based on surface characteristics of aggregates. *Materials*, 11 (9), 1488.

Tang, Q., *et al.*, 2021. Physical, chemical and interfacial properties of modified recycled concrete aggregates for asphalt mixtures: A review. *Construction and Building Materials*, 312, 125357.

Tanzadeh, R., and Shafabakhsh, G., 2020. Surface free energy and adhesion energy evaluation of modified bitumen with recycled carbon black (micro-nano) from gases and petrochemical waste. *Construction and Building Materials*, 245, 118361.

Thanaya, I.N.A., 2003. *Improving the performance of cold bituminous emulsion mixtures (cbems): incorporating waste materials*. Thesis (PhD). The University of Leeds.

Wang, Z., *et al.*, 2020. Adhesion improvement between rap and emulsified asphalt by modifying the surface characteristics of rap. *Advances in Materials Science and Engineering*, 2020, 1–10.

Wang, F., Liu, Y., and Hu, S., 2013. Effect of early cement hydration on the chemical stability of asphalt emulsion. *Construction and Building Materials*, 42, 146–151.

Wang, L., Shen, A., and Yao, J., 2020. Effect of different coarse aggregate surface morphologies on cement emulsified asphalt adhesion. *Construction and Building Materials*, 262, 120030.

Wates, J.M., and James, A.D., 1993. Zeta potential measurements on bitumen emulsions and road aggregates. *In*: A.D. James and J. Wates, ed., *Presented at the 1st World Congress on Emulsions*,19–22nd October 1993, Paris, France, 1-40-089.

Wei, J., and Zhang, Y., 2012. Application of sessile drop method to determine surface free energy of asphalt and aggregate. *Journal of Testing and Evaluation*, 40, 20120060.

Wu, S., *et al.*, 2020. Study of adhesion between crack sealant and pavement combining surface free energy measurement with molecular dynamics simulation. *Construction and Building Materials*, 240, 117900.

You, L., *et al.*, 2020. Stability and rheology of asphalt-emulsion under varying acidic and alkaline levels. *Journal of Cleaner Production*, 256, 120417.

Zhang, H., Wang, Z., and Wang, Q., 2020. Quantitative evaluation of cement emulsified asphalt mortar and aggregate adhesion performance with dynamic mechanical analysis. *Construction and Building Materials*, 262, 120043.

Ziyani, L., *et al.*, 2014. Chemical reactivity of mineral aggregates in aqueous solution: relationship with bitumen emulsion breaking. *Journal of Materials Science*, 49 (6), 2465–2476.

Ziyani, L., *et al.*, 2016. A predictive and experimental method to assess bitumen emulsion wetting on mineral substrates. *Colloids and Surfaces A: Physicochemical and Engineering Aspects*, 489, 322–335.